Korean J. Chem. Eng., 36(11), 1882-1889 (2019)
DOI: 10.1007/s11814-019-0387-7

pISSN: 0256-1115
eISSN: 1975-7220

Prolonged antimicrobial activity of silver core-carbon shell nanoparticles

Zengkai Wang*, Tianke Wang*, An Hua,***, Song Ma**,†, Zhidong Zhang**, and Lei Liu*,†**

*School of Materials Science and Engineering and Institute for Advanced Materials, Jiangsu University, Zhenjiang 212013, China
**Shenyang National Laboratory for Materials Science, Institute of Metal Research, Chinese Academy of Sciences, Shenyang 110016, China
***School of Materials Science and Engineering, University of Science and Technology of China, Hefei 230026, China
(*Received 9 June 2019 • accepted 10 September 2019*)

Abstract−Ag nanoparticles present good antimicrobial activity but with a potential toxicity to the cell, which limits the application. To address this issue, in this work, carbon-encapsulated sliver nanocapsules (Ag@C nanocapsules) were prepared by evaporating pure Ag ingot with the modified arc-discharge technique, and the Ag@C nanocapsules were acidified with nitric acid subsequently to facilitate the silver ion to release. Finally, Ag@C nanocapsules displayed a good and sustained antimicrobial activity against *E. coli* as a model of Gram-negative bacteria, due to the long-term release of sliver ions from Ag@C nanocapsules. The results obtained in this work indicate that the Ag@C nanocapsules may be a suitable nanomaterial for the bactericidal application.

Keywords: Antimicrobial Nanomaterials, Ag@C Nanocapsules, Carbon Shell, Sustained Release

INTRODUCTION

Over the last several decades, a variety of antibiotics have been widely used to fight bacterial infections, and have achieved considerable success. However, the abuse of antibiotics has also led to many serious side effects. For instance, the morphology of bacteria is preserved with the treatment of antibiotics, which leads to the drug resistance of bacteria [1]. Many promising approaches have been proposed to overcome the drug resistance of bacteria, such as antimicrobial peptides extracted from the plants, and insects can kill the bacteria without inducing drug resistance, but the stability and cytotoxicity of antimicrobial peptide gives a limitation of biomedical application [2,3]. Antimicrobial nanomaterials have been developed with the aim to obtain nonresistant, highly stable and effective antibacterial materials such as silver, gold, tin and copper nanomaterials, which have undergone a continuous process of evolution and still remain an intriguing space to improve [4-9].

Ag nanoparticles (AgNPs) are the first commercialized nanoparticles and show attractive properties, such as excellent electrical conductivity, chemical stability, antifungal, and bactericidal properties and also eliminate multidrug resistant bacteria. AgNPs are nowadays used as wide-spectrum antimicrobials in a variety of applications, such as cosmetics, textiles, wound dressings, detergents, dental work, catheters, and water filtration [10-13]. For example, biomedical products with AgNPs are typically used to prevent bacterial infections by accelerating wound healing [14,15]. Ag^+ and AgNPs have been reported to have remarkable antimicrobial properties against various pathogens including bacteria, fungi, and viruses [16-18]. In addition, AgNPs are more effective in killing gram-negative bacterial strains than gram-positive due to different cell wall structure between gram-positive and gram-negative bacteria [19,20]. Therefore, silver-based antimicrobial materials have attracted extensive attention for application in biomedicine and antibacterial devices [21,22]. Antibacterial activity of AgNPs prepared by various methods has been investigated on several bacterial strains [23-32]. AgNPs show good antibacterial activity in pure [23] and composite forms [24]. However, AgNPs present a potential toxicity due to direct contacting between AgNPs and cell membrane, which can increase the ROS to toxic level to the cell and facilitate the binding between AgNPs and proteins of cell. Furthermore, the slow oxidation and corrosion of unprotected AgNPs can also lead to increase of the concentration of Ag^+ ions to cell toxic level [33,34]. In vitro cell culture studies have showed toxic effects of AgNPs in immortal human skin keratinocytes, human erythrocytes, human neuroblastoma cells, human embryonic kidney cells, human liver cells, and human colon cells [35-37].

To address this issue, it is necessary to encapsulate AgNPs into other materials to prevent them directly contacting the human cell, and to control the release of Ag^+. In this aspect, AgNPs have been encapsulated in polymer matrix to form surface coatings [38,39]. However, the intense polymer will suppress the antibacterial effect and the aging of polymer layer also leads to the leaching of AgNPs and decreases the long-term antibacterial activity of AgNPs composites [40]. Other AgNPs based composite materials with the substitution of silk fibroin nanofibers [41], silica nanowires [42], carbon nanotube [40], zeolite clay [43], titanium dioxide [44], and other nanostructures [45,46], have been investigated. In comparison, carbon nanomaterials, which are non-toxic or low-toxic to organisms, have been demonstrated to have great promise in biomedicine [47,48]. Carbon material is an ideal coating material, which has a

†To whom correspondence should be addressed.
E-mail: liul@ujs.edu.cn, songma@imr.ac.cn

better stability and electrical conductivity than SiO_2, TiO_2 and other coating materials, and simultaneously can improve the biocompatibility between the composite materials and the organisms. The design of composite nanostructures with carbon shell and silver core has attracted attention due to the novel physicochemical [49, 50], especially, which can be applied in the bactericidal materials.

In the present study, we synthesized carbon-encapsulated sliver nanocapsules (Ag@C nanocapsules) by a modified arc-discharge technique as antibacterial agents, and then the Ag@C nanocapsules were acidified with nitric acid subsequently to increase the biocompatibility of materials and the affinity to the bacteria due to the introduction of carboxylic group, and also facilitate the Ag^+ to release. We aimed to construct the Ag@C nanocapsules with effective antibacterial activity, low cytotoxicity to human cell and the good affinity to bacteria. Actually, Ag@C nanocapsules displayed good and sustained antimicrobial activity against *Escherichia coli* (*E. coli*) as a model of Gram-negative bacteria, due to the long-term release of sliver ions from Ag@C nanocapsules. The designed silver based nanocomposites may be a suitable nanomaterial for bactericidal application.

METHODS

1. Preparation of Ag@C Nanocapsules

The Ag@C nanocapsules were prepared by evaporating pure Ag ingot with the modified arc-discharge technique. The Ag ingot with purity 99.99% was used as anode target, while a graphite needle with a diameter of 8 mm was served as cathode. As the vacuum of chamber reached 5×10^{-3} Pa, the argon and hydrogen with purity of 99.99% were introduced into the chamber to serve as the source of plasma, which led to an increase of 0.2 and 0.02 MPa in chamber pressure, respectively. Subsequently, 20 mL pure ethanol serving as the carbon source was introduced into the chamber. During the arc-discharging process, the Ag atoms were evaporated out from the Ag ingot to form the Ag nanoparticles, and then encapsulated by the carbon atoms decomposed from the ethanol to finally form the Ag@C nanocapsules [51].

2. Acidification of Ag@C Nanocapsules

First, a certain amount of Ag@C spheres was added to a beaker of 10 mL concentrated nitric acid (diluted 20 times), sonicated for 30 min. Then, the beaker was placed in a water bath heated to 60 °C in advance, and stirred at 60 °C for 30 min. Acidification was completed. It was washed three times with water and dried in an oven at 60 °C for 12 h. If no special explanation is given, the Ag@C nanocapsules are hereafter referred to as acidified Ag@C nanocapsules.

3. Antimicrobial Activity

The assessment of antibacterial activity of Ag@C nanocapsules against Gram-negative Bacterium *Escherichia coli*, was performed. *E. coli* culture was prepared using standard method and discussed in earlier reports [52]. Samples of 180 μL different concentration Ag@C nanocapsules were mixed with 20 μL of phosphate buffer saline (PBS) solution of *E. coli* bacterial suspensions (~10^7 CFU/mL), and then the blend solutions were shaken for different time. Finally, the bacterial suspension was diluted and cultured on agar plate to count the live bacteria cells. The inoculated agar plates were allowed to dry for 5 min, and then the sample without Ag@C nanocapsules was used as control. The agar plates were then incubated at 37 °C for 18 h.

4. Characterization

4-1. Scanning Electron Microscope (SEM)

The morphology of the Ag@C nanocapsules was examined using a JSM-7800F Thermal field emission SEM (JEOL, Akishima-shi, Japan). The Ag@C nanocapsules were suspended in deionized water and then subjected to sonication using a Scientz ultrasonic cell disruptor (model IID, Scientz, Zhejiang, China) at an energy output of 80% amplitude for 60 min, five microliters of the suspensions were directly dropped on the Si substrate. The samples were dried overnight and then sputtered with platinum.

4-2. Transmission Electron Microscope (TEM)

The morphology and microstructure characterization of products were performed by an HRTEM (Tecnai G2 F30 S-TWIN, FEI, Hillsboro, Oregon State, USA) with a double tilt holder operating at emission voltages of 200 kV.

4-3. X-ray Diffraction (XRD)

The crystal structure and phase of the Ag@C nanocapsules were carried out on an X-ray diffraction (Rigaku, Japan), at a scanning speed of 6.0° min^{-1} in the 2θ range from 10 to 80° (operated at 40 kV and 200 mA, Cu $K\alpha$ source).

4-4. Inductively Coupled Plasma Optical Emission Spectrometer (ICP-OES)

The Ag release of the samples was measured using ICP-OES (ICP-5000, FPI, China) by based on a standard curve obtained at the same condition.

4-5. Cell Morphological Change

SEM, and TEM were used to observe the morphological changes of the tested bacteria treated with Ag@C nanocapsules, and observe the interaction between bacteria and the Ag@C nanocapsules.

5. Cytotoxicity Test

Human hepatocellular liver carcinoma cells (HepG2) were grown (at 37 °C in a 5% CO_2 atmosphere) in Dulbecco's modified Eagle's medium (DMEM, Gibco, USA) supplemented with 10% fetal bovine serum (FBS, Gibco, USA). Cells were incubated for 24 h after exposure to AgNPs (around 100 nm) and Ag@C nanocapsules with different concentration (0, 10, 20, 40, 60, 120 μg/mL) in 96-well plates for the cell viability assay. The cell adhesive status was recorded using a microscope and the cell proliferative ability was evaluated using the Cell Counting Kit-8 (CCK-8; Beyotime Institute of Biotechnology, Haimen, China). 100 μL of the CCK-8 solution was added to each well, and the cells were incubated at 37 °C for 4 h. Absorbance was determined at 450 nm using a microplate spectrophotometer (BioTek, Winooski, VT, USA). Six parallel replicates were read for each sample.

RESULTS AND DISCUSSION

The Ag@C nanocapsules were prepared by evaporating pure Ag ingot to form the Ag nanoparticles and using pure ethanol served as the carbon shell with the modified arc-discharge technique, as shown in Schematic 1.

The Ag@C nanocapsules synthesized present nearly spherical morphology with smooth surface and broad particle size distribution 462 nm±240 nm (PdI=0.295) as shown in Fig. 1(a) and 1(b).

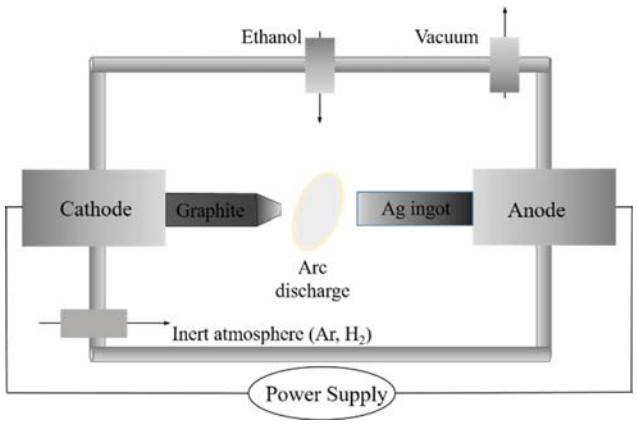

Schematic 1. Schematic representation of preparation of Ag@C nanocapsules through modified arc-discharge technique.

The AgNPs and coating layers were characterized by TEM, and the coating layers were determined to be graphite sheets tightly packed and ordered arranged to form an onion-like structure around the AgNPs (Fig. 1(c)). The silver core and carbon shell were observed clearly and the fringe spacing (0.235 nm) in the HRTEM image of Ag@C nanocapsules in the inset of Fig. 1(c) agreed with Ag (111) lattice plane reported in the JCPDS (No. 65-2871). The XRD of the Ag@C nanocapsules and the characterized diffraction peaks for corresponding crystalline planes are shown in Fig. 1(d). The major diffraction peaks at 38.11°, 44.28°, 64.43°, and 77.47° could be assigned to the (111), (200), (220) and (311) planes of the cubic Ag phase (JCPDS No. 65-2871), and no silver oxide peaks were observed, which can prove the existence of the single phase silver in the Ag@C nanocapsules. Indexed with carbon, the characteristic peak of C (001) was 22.34° which has relatively weak intensity in as-synthesized composites. We suggest that the content of AgNPs was relatively higher, leading to the diffraction signals of the carbon sheets probably being covered up by AgNPs. The breaking down of translational symmetry of the graphite in shell could also cause the weak peaks of the carbon sheets. Furthermore, no peaks corresponding to impurities were detected, and therefore, the graphite layers of Ag@C nanocapsules had almost no defects and no Ag crystals leaked out.

To improve the release efficiency of Ag^+ from protected AgNPs and increase the bactericidal activity, Ag@C nanocapsules were acidized with HNO_3. As shown in Fig. 2, after the acidification, the particle size decreased to be approximately 450 nm. Simultaneously, the surface of the Ag@C nanocapsules gradually became rough (Fig. 2(b)), and the thickness of graphite layers of nanocapsules decreased compared to the ones without the acidification (Fig. 1(c) and Fig. 2(b)), which indicated that the shell layer was disrupted by the acidification treatment. The increased percentage loading of Ag in EDX spectrum of the acidified Ag@C nanocapsules further verified that parts of AgNPs were exposed from the Ag@C nanocapsules (not show). In addition, local graphite layers were broken and the bare sliver was observed to expose as marked with red circles in Fig. 2(c); this method could avoid AgNPs direct contact with the cells and simultaneously could release silver ions. It suggests the release of Ag^+ could be accelerated from the AgNPs, and

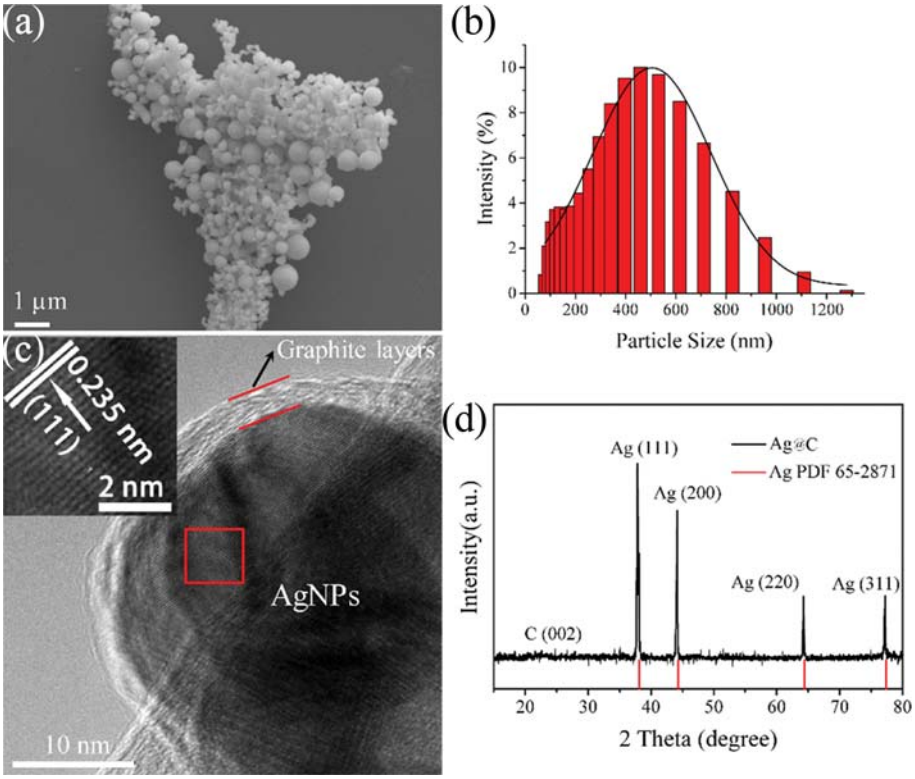

Fig. 1. Morphological characterization of Ag@C nanocapsules. (a) SEM image, (b) particle size distribution, (c) HRTEM image and (d) XRD spectra of the pristine Ag@C nanocapsules.

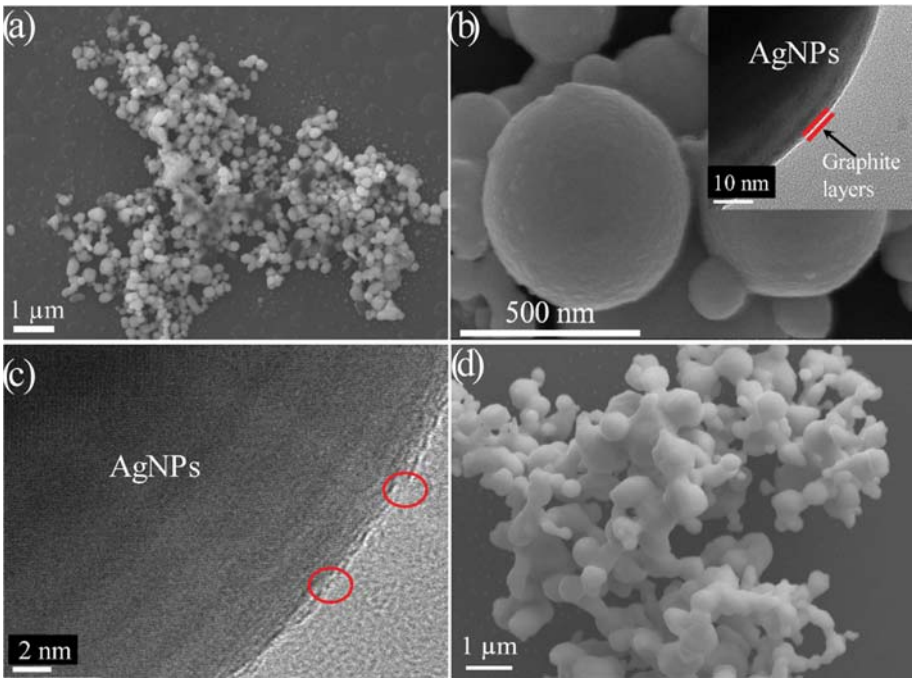

Fig. 2. SEM and TEM images of the Ag@C nanocapsules that were acidified with HNO_3. (a, b) SEM and (c) HRTEM images of acidified Ag@C nanocapsules (C_{HNO3}≈0.8 mol/L); (d) SEM image of acidified Ag@C nanocapsules (C_{HNO3}≈1.6 mol/L).

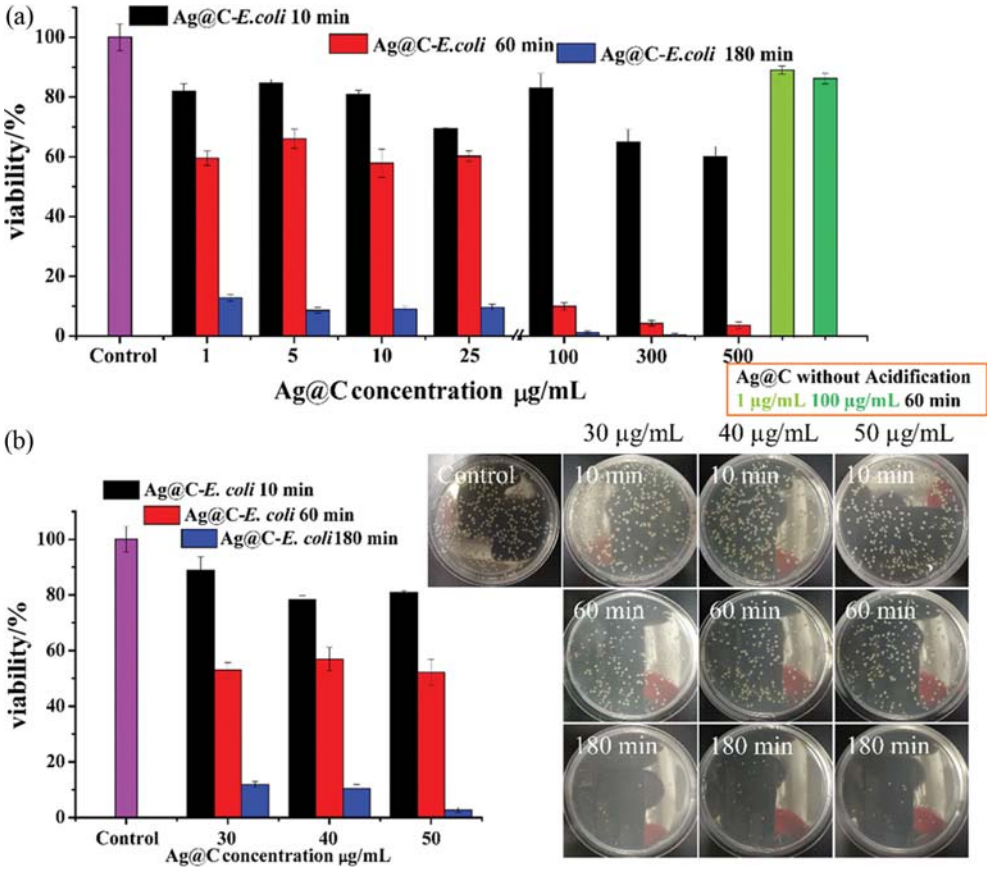

Fig. 3. Antibacterial activity of Ag@C nanocapsules against *E. coli*. (a) the viability of different concentrations of Ag@C nanocapsules against *E. coli*. (b) Inhibition of colonies after Ag@C nanocapsules (30 μg/mL, 40 μg/mL and 50 μg/mL) treated with different time (10 min, 60 min, 180 min).

the bactericidal efficiency could be enhanced. The acidification time and the concentration of HNO_3 could affect the morphology of Ag@C nanocapsules. With the increment of acidification time, the graphite layers could be destroyed and cause internal silver leakage (Fig. 2(c)). When excessive acidification is utilized, the graphite layers can be destroyed completely and make the AgNPs leak out completely, which has been proved by the long-time acidification or under the treatment of high concentration of HNO_3 (Fig. 2(d)).

To further evaluate the antibacterial activity of Ag@C nanocapsules, the acidified Ag@C nanocapsules with different concentrations (1, 5, 10, 25, 30, 40, 50, 100, 300 and 500 μg/mL, respectively) and Ag@C nanocapsules without acidification (1 μg/mL, 100 μg/mL) were prepared to test the viability of gram-negative *E. coli* as model bacteria. The present study was performed using colony count method. As shown in Fig. 3(a), the antibacterial activity of the Ag@C nanocapsules with and without the acidification was tested against the *E. coli* at the same concentration (1 μg/mL, 100 μg/mL), and it was found that the Ag@C nanocapsules without acidification were almost inefficient in killing *E. coli*, although incubated 60 min under shaking condition and followed by spread plating for 18 h. The bacterial viability was still 93% for 1 μg/mL and 85% for 100 μg/mL, and it was probably due to the onion-like structure of Ag@C nanocapsules, and the Ag^+ ions were difficult to diffuse through the thicker graphite layers. The 58% viability of *E. coil* is acquired for the acidified Ag@C nanocapsules with the concentration of 500 μg/mL after the 10 min incubation with *E. coli*. At the same concentration, the viability of bacteria decreased obviously with the increment of incubation time (10 min, 60 min and 180 min). In the concentration range of Ag@C nanocapsules we tested, the bacterial killing rate was low at the initial stage, and it could almost kill the bacteria in 3 hours. The bacteria cannot be killed completely at low concentration of Ag@C (below 25 μg/mL). We further tested the antimicrobial activity of Ag@C, and found that Ag@C with the concentration of 50 μg/mL could kill the bacteria completely after 3 h incubation (Fig. 3(b)). Generally, we proposed a strategy of AgNPs construction to optimize the antimicrobial activity and increase the biocompatibility of AgNPs.

The size and the specific surface area do affect the antibacterial activity of AgNPs [53]. The previous study showed that silver ion (Ag^+) [54,55] and Ag^0 both make a contribution to the bactericidal activity. To improve the antimicrobial activity of AgNPs to bacteria, facilitating the releasing silver ions from AgNPs is an efficient way [56], and enhancing the interaction of AgNPs to the bacterial cell is also considered as a good option, such as electrostatic interaction between the positive charged AgNPs and negative charged bacterial cells [57,58]. We compared the antimicrobial activity of Ag@C nanocapsules with reported AgNPs of the literature [47,59], Sondi et al. prepared the AgNPs with particle size of 12.3±4.2 nm, and studied the antimicrobial activity of AgNPs against the *E. coli* through approximately 10^5 CFU of *E. coli* were cultured on LB agar plates supplemented with AgNPs in concentrations of 10-100 μg/mL. The results showed that the AgNPs at a concentration of 10 μg/mL could inhibit bacterial growth by 70%, and the concentration of 50-60 μg/mL caused 100% inhibition of bacterial growth.

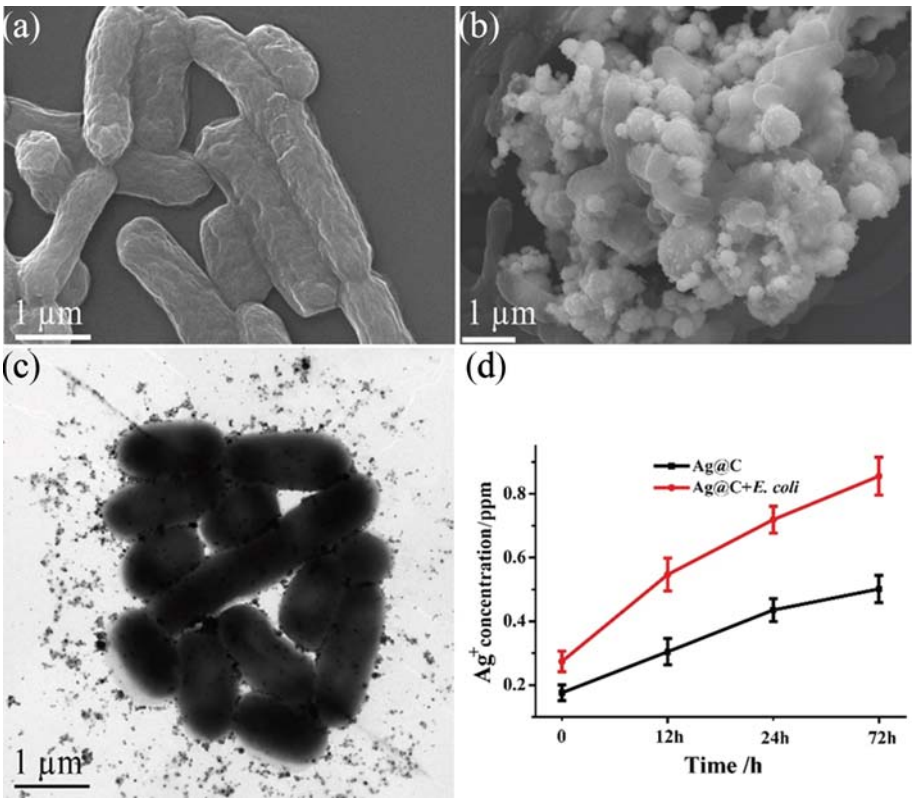

Fig. 4. SEM and TEM images of *E. coli.* incubated with Ag@C nanocapsules (50 μg/mL). (a) pristine *E. coli*; (b), (c) The blend solutions of Ag@C nanocapsules and *E. coli*; (d) Ag^+ concentration of Ag@C nanocapsules solutions before and after addition of *E. coli*.

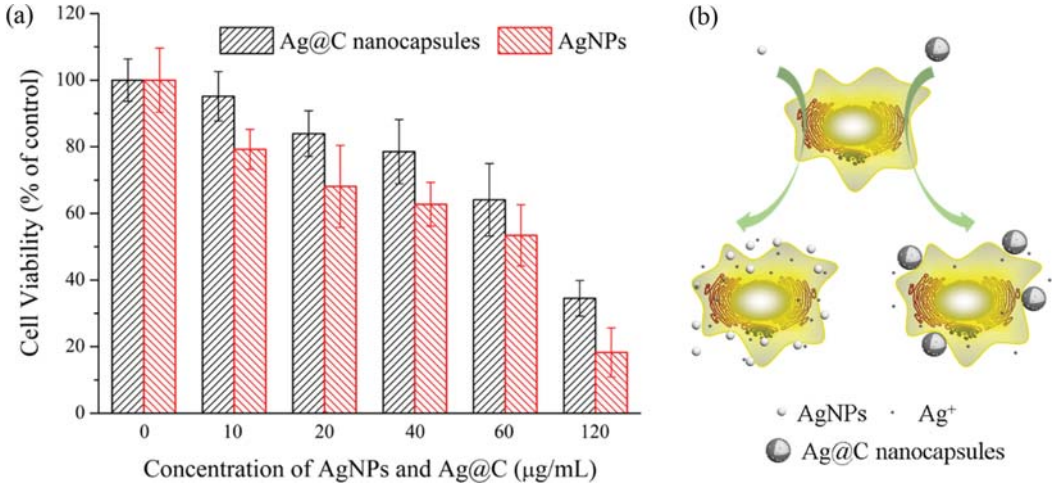

Fig. 5. (a) The Cell viability determined by CCK-8 assay after exposure to AgNPs and Ag@C nanocapsules at the indicated times. Data expressed as mean±SD, n=6. (b) Schematic of interaction of between cell and AgNPs and Ag@C nanocapsules.

The number of bacterial colonies grown on LB plates with more than 5 μg/mL of Ag@C nanocapsules treated with 180 min could inhibit bacterial growth by 80%. Although the method was slightly different, the antimicrobial activity of Ag@C nanocapsules and AgNPs was almost the same. In addition, it was reported that the cytotoxicity of AgNPs has been reported to be a dose-, size- and time-dependent manner [60], the larger Ag@C nanocapsules could reduce endocytosis to reduce cytotoxicity and also show good antimicrobial activity.

Although AgNPs have remarkable antimicrobial properties, however, the bactericidal mechanisms of AgNPs remain unclear. There is an ongoing debate over whether AgNPs or Ag^+ exert a cytotoxic effect on microorganisms [61,62]. In this work, carbon surface of Ag@C nanocapsules was modified by nitric acid to introduce carbonyl and carboxylic groups [63,64]. As shown in Fig. 4(b)-4(c), the acidified Ag@C dispersed well on the surface of the bacteria, and the carboxyl or carbonyl on the graphite layer of AgNPs could bind to the surface of bacteria. Meanwhile, the acidification of Ag@C nanocapsules could oxidize the graphite layer of AgNPs as well as the AgNPs, which facilitates silver ions released from the surface of AgNPs, and further disturbs various metabolic pathways, inhibits bacterial reproduction and finally causes bacterial death. The literature reported that the electrostatic attraction between the negatively charged cell wall of *E. coli* and positively charged silver ions is key to bactericidal activity [19]. Due to the coating of graphite layers, the AgNPs were oxidized slowly, and released silver ions for a long-term. The concentration of Ag^+ ions increased obviously with the increment of time, after the addition of *E. coli* in Fig. 4(d), which led to the increased contact-active antibacterial activity. The long-term antimicrobial activity of Ag@C was proved in Fig. 4(d) from 0 h to 72 h, because more silver ions released from Ag@C nanocapsules, compared to the silver concentration without the bacteria. Therefore, we could finally speculate that Ag@C nanocapsules were distributed around bacteria through the interaction between the bacteria and acidified graphite layer of Ag@C nanocapsules, and a similar mechanism causes the degradation of the membrane structure of *E. coli* during the treatment with AgNPs [65].

The toxicity of Ag@C nanocapsules and pure AgNPs was evaluated in HepG2 cell, with the objective to compare the difference of cytotoxicity between Ag@C nanocapsules and AgNPs (Fig. 5). HepG2 cell line maintains many specialized functions of normal liver parenchymal cells, which represent the possible influence when AgNPs or Ag@C nanocapsules enter the blood system. The results of CCK-8 assays showed a dose-dependent decrease in viability percentage of HepG2 cell after 24 h exposure to Ag@C nanocapsules and AgNPs. Similarly, there is much debate in the literature on whether AgNPs or silver ions exert toxic effects in mammalian cells. However, Ag@C nanocapsules have shown higher cell viability than pure AgNPs at each concentration, and AgNPs were encapsulated into carbon shell to prevent them direct contacting with the human cell. It indicated that this method could reduce the toxicity of Ag@C nanocapsules to some extent and also show the antimicrobial activity. As shown in Fig. 5(b), conventional AgNPs will be swallowed by cells and enter the cell interior, excessive silver nanoparticles and silver ions will produce cytotoxicity. While Ag@C nanocapsules will hardly be swallowed by cells. Moreover, the carbon layer will prevent the direct contact between silver nanoparticles and cells, and reduce cell phagocytosis and cytotoxicity.

CONCLUSION

We prepared Ag@C nanocapsules by the modified arc-discharge technique and the surface acidification to control the release of Ag^+ in the Ag@C nanocapsules and increase the solubility of nanomaterials. Ag@C nanocapsules presented a good and sustained antimicrobial activity against *E. coli* as a model of Gram-negative bacteria, due to the long-term release of sliver ions from Ag@C nanocapsules. This work may make possible advances in the formulation of new type of antimicrobial materials and can be applied in bioscience and biomedicine.

ACKNOWLEDGEMENTS

We acknowledge the financial sponsorship by the National Nat-

ural Science Foundation of China (51571195, 51871219, 51590883), We also gratefully acknowledge support of the National Key R&D Program of China (No. 2017YFA0206301).

NOMENCLATURE

Symbols

C : concentration
°C : degree centigrade
h : hour
mg : milligram
μg : microgramme
mL : milliliter
mmoL: millimole
moL : moore

Abbreviations

Ag@C nanocapsules : carbon-encapsulated metallic sliver nanocapsules
AgNPs : Ag nanoparticles
SEM : scanning electron microscopy
HRTEM : high resolution transmission electron microscope
XRD : X-ray diffraction
ICP-OES : inductively coupled plasma optical emission spectrometer

REFERENCES

1. G. Taubes, *Science*, **321**, 356 (2008).
2. L. C. Huang, S. Narayanan, R. L. Redfern and A. M. Mcdermott, *Invest. Ophthalmol. Vis. Sci.*, **43**, 82 (2002).
3. M. M. Javadpour, M. M. Juban, W.-C. J. Lo, S. M. Bishop, J. B. Alberty, S. M. Cowell, C. L. Becker and M. L. Mclaughlin, *J. Med. Chem.*, **39**, 3107 (1996).
4. L. a. T. W. Asri, M. Crismaru, S. Roest, Y. Chen, O. Ivashenko, P. Rudolf, J. C. Tiller, H. C. Van Der Mei, T. J. A. Loontjens and H. J. Busscher, *Adv. Funct. Mater.*, **24**, 346 (2014).
5. M. Kazemzadeh-Narbat, B. F. Lai, C. Ding, J. N. Kizhakkedathu, R. E. Hancock and R. Wang, *Biomaterials*, **34**, 5969 (2013).
6. C. J. Waschinski, J. Zimmermann, U. Salz, R. Hutzler, G. Sadowski and J. C. Tiller, *Adv. Mater.*, **20**, 104 (2008).
7. A. Makovitzki, D. Avrahami and Y. Shai, *Proc. Natl. Acad. Sci. U.S.A.*, **103**, 15997 (2006).
8. A. Zumbuehl, L. Ferreira, D. Kuhn, A. Astashkina, L. Long, Y. Yeo, T. Iaconis, M. Ghannoum, G. R. Fink, R. Langer and D. S. Kohane, *Proc. Natl. Acad. Sci. U.S.A.*, **104**, 12994 (2007).
9. S. Pritz, M. Patzel, G. Szeimies, M. Dathe and M. Bienert, *Org. Biomol. Chem.*, **5**, 1789 (2007).
10. J. K. Pandey, R. K. Swarnkar, K. K. Soumya, P. Dwivedi, M. K. Singh, S. Sundaram and R. Gopal, *Appl. Biochem. Biotechnol.*, **174**, 1021 (2014).
11. N. Zafar, S. Shamaila, J. Nazir, R. Sharif, M. S. Rafique, J. Ul-Hasan, S. Ammara and H. Khalid, *J. Mater. Sci. Technol.*, **32**, 721 (2016).
12. C. Wang, S. Wu, M. Jian, J. Xie, L. Xu, X. Yang, Q. Zheng and Y. Zhang, *Nano Res.*, **9**, 1 (2016).
13. X.-C. Ma, Y. Dai, L. Yu and B.-B. Huang, *Light: Science & Amp; Applications*, **5**, e16017 (2016).
14. C. Rigo, L. Ferroni, I. Tocco, M. Roman, I. Munivrana, C. Gardin, W. R. L. Cairns, V. Vindigni, B. Azzena, C. Barbante and B. Zavan, *Int. J. Mol. Sci.*, **14**, 4817 (2013).
15. X. Liu, P.-Y. Lee, C.-M. Ho, V. C. H. Lui, Y. Chen, C.-M. Che, P. K. H. Tam and K. K. Y. Wong, *ChemMedChem*, **5**, 468 (2010).
16. S. Chernousova and M. Epple, *Angew. Chem. Int. Ed.*, **52**, 1636 (2013).
17. J. A. Spadaro, T. J. Berger, S. D. Barranco, S. E. Chapin and R. O. Becker, *Antimicrob. Agents Chemother.*, **6**, 637 (1974).
18. Rahisuddin, S. A. Al-Thabaiti, Z. Khan and N. Manzoor, *Bioprocess Biosystems Eng.*, **38**, 1773 (2015).
19. Y. N. Slavin, J. Asnis, U. O. Häfeli and H. Bach, *J. Nanobiotechnol.*, **15**, 65 (2017).
20. E. E. Fröhlich and E. Fröhlich, *Int. J. Mol. Sci.*, **17**, 509 (2016).
21. K. S. Siddiqi, A. Husen and R. a. K. Rao, *J. Nanobiotechnol.*, **16**, 14 (2018).
22. M. C. G. R. D. G. Marotta, *J. Mater. Sci. - Mater. Med.*, **15**, 831 (2004).
23. L. F. Espinosa-Cristóbal, G. A. Martínez-Castañón, R. E. Martínez-Martínez, J. P. Loyola-Rodríguez, N. Patiño-Marín, J. F. Reyes-Macías and F. Ruiz, *Mater. Lett.*, **63**, 2603 (2009).
24. G. A. Sotiriou and S. E. Pratsinis, *Environ. Sci. Technol.*, **44**, 5649 (2010).
25. X. L. Cao, C. Cheng, Y. L. Ma and C. S. Zhao, *J. Mater. Sci. - Mater. Med.*, **21**, 2861 (2010).
26. S. Kaviya, J. Santhanalakshmi, B. Viswanathan, J. Muthumary and K. Srinivasan, *Spectroc. Acta Pt. A-Molec. Biomolec. Spectr.*, **79**, 594 (2011).
27. M. Kawashita, S. Tsuneyama, F. Miyaji, T. Kokubo, H. Kozuka and K. Yamamoto, *Biomaterials*, **21**, 393 (2000).
28. S. Pal, Y. K. Tak and J. M. Song, *Appl. Environ. Microbiol.*, **73**, 1712 (2007).
29. S. Jaiswal, B. Duffy, A. K. Jaiswal, N. Stobie and P. Mchale, *Int. J. Antimicrob. Agents*, **36**, 280 (2010).
30. A. Travan, C. Pelillo, I. Donati, E. Marsich, M. Benincasa, T. Scarpa, S. Semeraro, G. Turco, R. Gennaro and S. Paoletti, *Biomacromolecules*, **10**, 1429 (2009).
31. A. J. Kora, R. Manjusha and J. Arunachalam, *Mater. Sci. Eng., C*, **29**, 2104 (2009).
32. X. Xu, Q. Yang, Y. Wang, H. Yu, X. Chen and X. Jing, *Eur. Polym. J.*, **42**, 2081 (2006).
33. P. Hartemann, P. Hoet, A. Proykova, T. Fernandes, A. Baun, W. De Jong, J. Filser, A. Hensten, C. Kneuer, J.-Y. Maillard, H. Norppa, M. Scheringer and S. Wijnhoven, *Mater. Today*, **18**, 122 (2015).
34. P. Dubey, I. Matai, S. U. Kumar, A. Sachdev, B. Bhushan and P. Gopinath, *Adv. Colloid Interface Sci.*, **221**, 4 (2015).
35. J. Carrola, V. Bastos, I. Jarak, R. Oliveira-Silva, E. Malheiro, A. L. Daniel-Da-Silva, H. Oliveira, C. Santos, A. M. Gil and I. F. Duarte, *Nanotoxicology*, **10**, 1105 (2016).
36. S. C. Sahu, J. Zheng, L. Graham, L. Chen, J. Ihrie, J. J. Yourick and R. L. Sprando, *J. Appl. Toxicol.*, **34**, 1155 (2014).
37. X. Jiang, C. Lu, M. Tang, Z. Yang, W. Jia, Y. Ma, P. Jia, D. Pei and H. Wang, *Acs Omega*, **3**, 6770 (2018).
38. S. Chernousova and M. Epple, *Angew. Chem. Int. Ed. Engl.*, **52**, 1636 (2013).
39. T. S. Sileika, H. D. Kim, P. Maniak and P. B. Messersmith, *ACS Appl. Mater. Interfaces*, **3**, 4602 (2011).

40. C. Nie, Y. Yang, C. Cheng, L. Ma, J. Deng, L. Wang and C. Zhao, *Acta Biomater.*, **51**, 479 (2017).
41. P. Li, Z. Jia, Q. Wang, P. Tang, M. Wang, K. Wang, J. Fang, C. Zhao, F. Ren, X. Ge and X. Lu, *J. Mater. Chem. B*, **6**, 7427 (2018).
42. M. Lv, S. Su, Y. He, Q. Huang, W. Hu, D. Li, C. Fan and S. T. Lee, *Adv. Mater.*, **22**, 5463 (2010).
43. K. A. Rieger, H. J. Cho, H. F. Yeung, W. Fan and J. D. Schiffman, *ACS Appl. Mater. Interfaces*, **8**, 3032 (2016).
44. L. Zhao, H. Wang, K. Huo, L. Cui, W. Zhang, H. Ni, Y. Zhang, Z. Wu and P. K. Chu, *Biomaterials*, **32**, 5706 (2011).
45. H. Kong and J. Jang, *Langmuir*, **24**, 2051 (2008).
46. J. Song, H. Kang, C. Lee, S. H. Hwang and J. Jang, *ACS Appl. Mater. Interfaces*, **4**, 460 (2012).
47. M. Ahamed, M. S. Alsalhi and M. K. Siddiqui, *Clin. Chim. Acta*, **411**, 1841 (2010).
48. B. S. Harrison and A. Atala, *Biomaterials*, **28**, 344 (2007).
49. C. H. Tao, T. Chen, F. Ma, H. Liu, X. Li and S. Lin, *J. Nanosci. Nanotechnol.*, **19**, 2211 (2019).
50. Y. Qi, T.-Y. Xing, J. Zhao, G.-J. Weng, J.-J. Li, J. Zhu and J.-W. Zhao, *J. Alloys Compd.*, **776**, 934 (2019).
51. H. Wang, Y. Y. Dai, D. Y. Geng, S. Ma, D. Li, J. An, J. He, W. Liu and Z. D. Zhang, *Nanoscale*, **7**, 17312 (2015).
52. A. K. Karumuri, D. P. Oswal, H. A. Hostetler and S. M. Mukhopadhyay, *Mater. Lett.*, **109**, 83 (2013).
53. O. Choi and Z. Hu, *Environ. Sci. Technol.*, **42**, 4583 (2008).
54. M. Jose Ruben, E. Jose Luis, C. Alejandra, H. Katherine, J. B. Kouri, R. Jose Tapia and Y. Miguel Jose, *Nanotechnology*, **16**, 2346 (2005).
55. K. B. Holt and A. J. Bard, *Biochemistry*, **44**, 13214 (2005).
56. G. A. Sotiriou, A. Meyer, J. T. N. Knijnenburg, S. Panke and S. E. Pratsinis, *Langmuir*, **28**, 15929 (2012).
57. T. Hamouda and J. R. Baker, Jr., *J. Appl. Microbiol.*, **89**, 397 (2000).
58. I. Sondi and B. Salopek-Sondi, *J. Colloid Interface Sci.*, **275**, 177 (2004).
59. A. Shahzad, H. Saeed, M. Iqtedar, S. Z. Hussain, A. Kaleem, R. Abdullah, S. Sharif, S. Naz, F. Saleem, A. Aihetasham and A. Chaudhary, *J. Nanomater.*, **2019**, 14 (2019).
60. C. Liao, Y. Li and S. C. Tjong, *Int. J. Mol. Sci.*, **20**, 449 (2019).
61. G. Gahlawat, S. Shikha, B. S. Chaddha, S. R. Chaudhuri, S. Mayilraj and A. R. Choudhury, *Microb. Cell Fact*, **15**, 25 (2016).
62. R. Behra, L. Sigg, J. D. Clift Martin, F. Herzog, M. Minghetti, B. Johnston, A. Petri-Fink and B. Rothen-Rutishauser, *J. Royal Society Interface*, **10**, 20130396 (2013).
63. Y. F. Jia, C. J. Steele, I. P. Hayward and K. M. Thomas, *Carbon*, **36**, 1299 (1998).
64. M. L. Toebes, J. M. P. Van Heeswijk, J. H. Bitter, A. Jos Van Dillen and K. P. De Jong, *Carbon*, **42**, 307 (2004).
65. N. A. Amro, L. P. Kotra, K. Wadu-Mesthrige, A. Bulychev, S. Mobashery and G.-Y. Liu, *Langmuir*, **16**, 2789 (2000).